States of Water in Non-Equilibrium Glassy Polymers

ARTICLE · MARCH 2013

READS
21

2 AUTHORS, INCLUDING:

Eric M. Davis
Clemson University
16 PUBLICATIONS **81** CITATIONS

SEE PROFILE

THE JOURNAL OF PHYSICAL CHEMISTRY B

Article

pubs.acs.org/JPCB

Water Clustering in Glassy Polymers

Eric M. Davis and Yossef A. Elabd*

Department of Chemical and Biological Engineering, Drexel University, Philadelphia, Pennsylvania 19104, United States

ABSTRACT: In this study, water solubility and water clustering in several glassy polymers, including poly(methyl methacrylate) (PMMA), poly(styrene) (PS), and poly(vinylpyrrolidone) (PVP), were measured using both quartz spring microbalance (QSM) and Fourier transform infrared-attenuated total reflectance (FTIR-ATR) spectroscopy. Specifically, QSM was used to determine water solubility, while FTIR-ATR spectroscopy provided a direct, molecular-level measurement of water clustering. The Flory–Huggins theory was employed to obtain a measure of water-polymer interaction and water solubility, through both prediction and regression, where the theory failed to predict water solubility in both PMMA and PVP. Furthermore, a comparison of water clustering between direct FTIR-ATR spectroscopy measurements and predictions from the Zimm–Lundberg clustering analysis produced contradictory results. The failure of the Flory–Huggins theory and Zimm–Lundberg clustering analysis to describe water solubility and water clustering, respectively, in these glassy polymers is in part due to the equilibrium constraints under which these models are derived in contrast to the nonequilibrium state of glassy polymers. Additionally, FTIR-ATR spectroscopy results were compared to temperature-dependent diffusivity data, where a correlation between the activation energy for diffusion and the measured water clustering was observed.

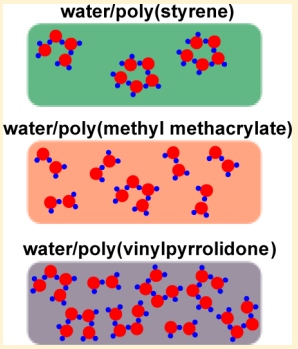

INTRODUCTION

Water sorption and diffusion in glassy polymers is of interest in many fields including drug delivery,[1] water desalination,[2,3] fuel cells,[4] food packaging,[5] and, more recently, in the pharmaceutical and contact lens industries.[6−8] Difficulties can arise when attempting to accurately measure water sorption and diffusion in glassy polymers due to the nonequilibrium state of the polymer (i.e., the glass transition temperature of the polymer is higher than the experimental temperature). This nonequilibrium state results in non-Fickian diffusion behavior, where concentration-gradient-driven diffusion of water in the polymer is often accompanied by a time-dependent, stress-induced relaxation of the polymer chains, allowing for continuous, gradual additional uptake of water at extended experimental times.[9−13] Furthermore, water sorption and diffusion in glassy polymers can be affected by water clustering that can occur in the polymer during the transport process. Therefore, deeper insight into water solubility and diffusivity and water clustering in glassy polymers are of interest.

The most commonly used method to determine the extent of clustering in a two-component polymer/solvent mixture was first introduced by Zimm and Lundberg.[14,15] This analysis method has been used as an indirect method of determining clustering (water cluster size) in a number of water/polymer mixtures.[7,8,16−23] The benefit of this analysis method is that the extent of solvent clustering can be mathematically determined directly from equilibrium solubility data. Recently, Prausnitz and co-workers[7,8] investigated the sorption and diffusion of water in a number of glassy polymers (e.g., poly(methyl methacrylate) (PMMA), poly(acrylonitrile) (PAN), poly(acrylic acid) (PAA)). In their study, the water sorption isotherms in these glassy polymers were used to determine the extent of clustering in each polymer using both the Zimm–Lundberg clustering analysis, as well as information obtained from the Flory–Huggins theory. The presence of self-associated water clusters in glassy polymers with low water solubilities (i.e., <2 wt %) was attributed to the high hydrophobicity of these polymers, where it is commonly thought that this hydrophobicity leads to a higher tendency of water molecules to self-associate.[24] It was also observed that water diffusivity in both PMMA and PAN was weakly dependent on concentration, while diffusion coefficients in PVP showed a strong correlation to water concentration, which was attributed to the fact that PVP sorbs more water than PMMA and PAN (i.e., free-volume effects) and is plasticized by water at high water vapor activities. The results of this study indicate that the absolute water solubility, along with water clustering, plays a critical role in understanding the fundamental transport mechanisms in glassy polymers.

Even more recently, Du et al.[23] studied the clustering of water in polylactide (PLA) with the Zimm–Lundberg clustering function, where it was determined that water molecules did not self-associate below water vapor activities of ca. 0.45, but the presence of larger, hydrogen-bonded water clusters were observed at higher activities. Later, in a separate independent study, Davis et al.[25] verified water clustering present in PLA spectroscopically, where dimers were observed at water vapor activities below ca. 0.65 and larger cluster sizes were observed at higher activities. In another recent study by Metz et al.,[26] water clustering in a poly(ethylene oxide)-*b*-poly(butylene terephthalate) block copolymer was studied, where good agreement between the Zimm–Lundberg analysis

Received: May 31, 2013
Revised: August 19, 2013
Published: August 20, 2013

and water cluster size obtained from FTIR-ATR spectroscopy was obtained. To our knowledge, this is one of a few reports where the Zimm−Lundberg clustering analysis was used as a complementary analysis technique to a more direct, molecular-level measurement technique. One drawback to the exclusive use of the Zimm−Lundberg model is that it only infers the extent of clustering in a polymer/solvent mixture from the equilibrium sorption data and is not a direct measurement of water clustering in the polymer. Other investigators have directly studied water clustering in nonequilibrium glassy polymers,[27−29] where the entire water O−H stretching region was deconvoluted into a number of different populations of water cluster sizes with varying strengths of self-association. More investigations that provide a direct measure of water clustering in glassy polymers in conjunction with models, such as the Zimm-Lundberg model, will be of great interest to providing a deeper understanding of water transport mechanisms in glassy polymers.

In this study, water sorption and diffusion was measured in three glassy polymers, including poly(methyl methacrylate) (PMMA), poly(vinylpyrrolidone) (PVP), and poly(styrene) (PS), using quartz spring microbalance (QSM) over a wide range of water vapor activity at a number of experimental temperatures. The water solubility data were analyzed with the Flory−Huggins theory and the Zimm−Lundberg clustering function to predict water solubility and water clustering, respectively, in these glassy polymers. Additionally, in situ Fourier transform infrared-attenuated total reflectance (FTIR-ATR) spectroscopy was employed to gain a direct measurement of water clustering present in the glassy polymers. In addition, infrared spectroscopy results were compared to temperature-dependent diffusivity data to help elucidate the impact of water clustering on sorption and diffusion.

EXPERIMENTAL SECTION

Materials. Poly(methyl methacrylate) (PMMA) (M_w = 100 000 g/mol, atactic) was purchased from Polysciences, Inc. Poly(vinyl pyrrolidone) (PVP) (M_w = 360 000 g/mol) and poly(styrene) (PS) (M_w = 190 000 g/mol) were purchased from Scientific Polymer Products, Inc. Tetrahydrofuran (THF) (anhydrous, ≥99.9%, inhibitor free) and toluene (ACS reagent, ≥99.5%) were purchased from Sigma-Aldrich. Ultrapure deionized water (resistivity ca. 16 MΩ·cm) was used for all sorption experiments.

Film Preparation. PMMA/THF, PVP/water, and PS/toluene solutions were produced by dissolving each polymer in their respective solvent at 5% w/w and mixing for 24 h to ensure a clear, homogeneous solution. Polymer film fabrication consisted of solution casting each solution onto a Teflon Petri dish to produce free-standing films for gravimetric experiments or solution casting onto the ATR crystal surface for FTIR-ATR spectroscopy experiments. After solution casting onto the appropriate surface for 24 h (PMMA film) and 72 h (PS film) in a fume hood, the PMMA and PS films were subsequently held under vacuum for an additional 24 h at room temperature (ca. 25 °C). Following this, the PMMA and PS films were annealed at 70 °C under vacuum for 3 h and then the temperature was increased to 120 °C and held under vacuum for an additional 3 h. PVP films were annealed at 100 °C under vacuum for 3 h after 48 h solution casting and then the temperature was increased to 200 °C for an additional hour while under vacuum. Note that all polymers were annealed above their glass transition temperature (T_g = 119, 181, and 101 °C for PMMA, PVP, and PS, respectively).[8,30] After annealing, all films were immediately stored in a desiccator prior to sorption experiments. Immediately following each sorption experiment, the thickness of each polymer film was measured using a digital micrometer (Mitutoyo) with a 1 μm accuracy, with the exception of the PVP films, where film thickness was measured prior to the start of each sorption experiment. Each film thickness was an average of at least three individual measurements at different positions along the length of the film.

Quartz Spring Microbalance. A glassy polymer film (ca. 50 mg), along with metal reference (ca. 15 mg), was placed at the end of a vertical quartz spring (purchased from DeerSlayer Springs; 100 mg max load with 500 mm max extension; spring constant, k_{spring} = 0.98 g/s^2), which was housed inside a temperature-controlled glass column connected to a vapor sorption apparatus.[31] The entire vapor sorption apparatus, including glass column, along with a temperature-controlled reservoir, was completely evacuated of moisture and air via vacuum for at least 2 h. After the system was completely evacuated, the valve connecting the glass column (housing the quartz spring and sample) to the rest of the vapor sorption apparatus was closed (leak rate less than 0.5 mmHg/day). The reservoir containing deionized water was subjected to a number of freeze−pump−thaw vacuum cycles in order to remove all dissolved gases from the liquid. Pure water vapor was then charged into the temperature-controlled reservoir at specific vapor pressures, where it was allowed to equilibrate with the temperature of the jacket until steady-state was reached (i.e., the pressure transducer reading was constant). Once steady-state was reached, the valve separating the reservoir from the glass column was fully opened, exposing the polymer film in the glass column to a specified vapor pressure of water. The change in the extension of the spring due to water sorbing into the polymer was measured as a function of time with a high-speed charge coupled device (CCD) camera (DVT SmartImage Sensor; Series 600 model 630). The mass of water sorbed in the polymer was calculated from this spring extension data with the use of the spring constant and a force balance, that is, $F = mg = kx$. The water diffusion coefficient was obtained from regressing the experimental data (mass versus time) to a solution to Fick's second law. The solution is obtained by solving the one-dimensional continuity equation for a film in rectangular coordinates with the appropriate initial and boundary conditions for this experiment. For the case of the QSM gravimetric experiment, the following equation in terms of mass can be used to calculate the water diffusion coefficient:[32]

$$\frac{M(t)}{M_{eq}} = 1 - \sum_{n=0}^{\infty} \frac{8}{(2n+1)^2\pi^2} \exp\left[\frac{-D(2n+1)^2\pi^2 t}{4L^2}\right] \quad (1)$$

where $M(t)$ and M_{eq} denote the total amount of water that diffuses into the polymer film at time t and at equilibrium, respectively, and D is the diffusion coefficient of water. Therefore, the QSM gramivetric data can be regressed to eq 1 to determine D, which is the only adjustable parameter in this model. More details about this apparatus and procedures can be found elsewhere.[25,31]

FTIR-ATR Spectroscopy. Water in the polymer was also examined with infrared spectroscopy using an FTIR spectrometer (Nicolet 6700 Series; Thermo Electron) equipped

dx.doi.org/10.1021/jp405388d | J. Phys. Chem. B 2013, 117, 10629−10640

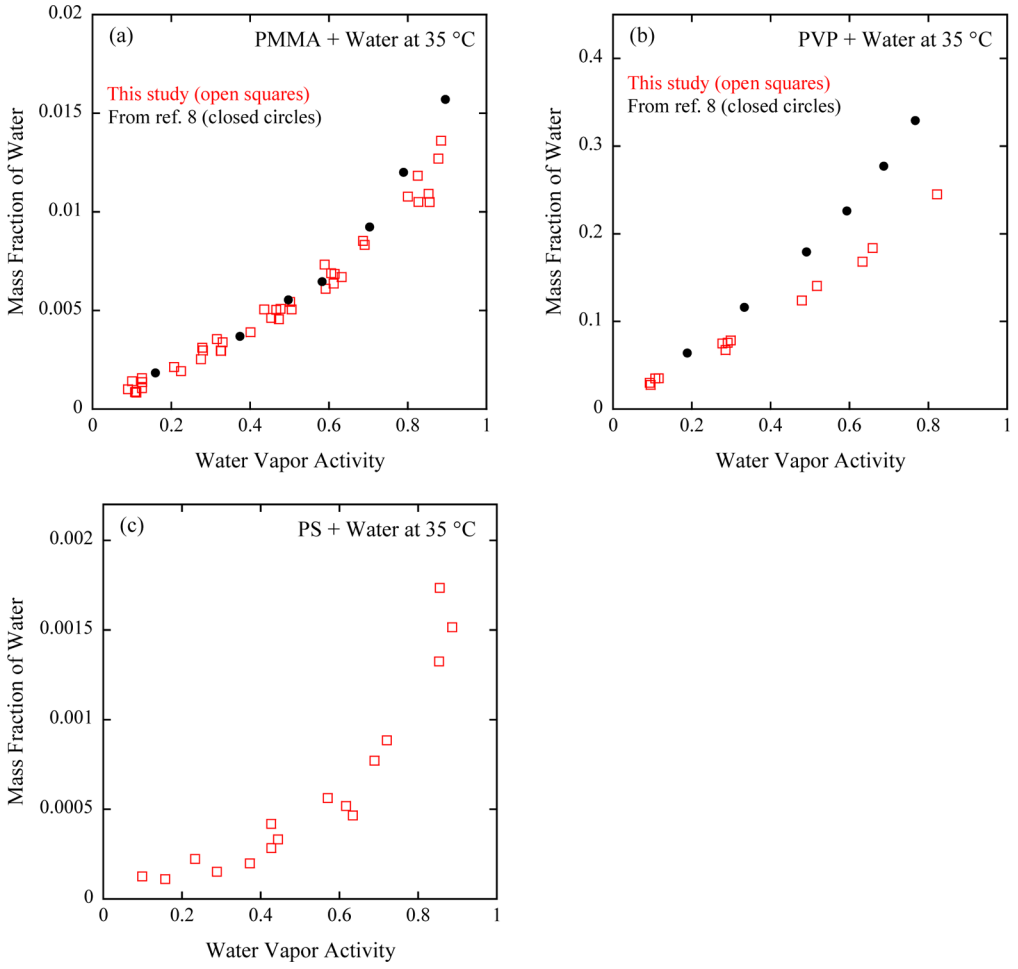

Figure 1. Sorption isotherms of water in (a) PMMA, (b) PVP, and (c) PS using QSM at 35 °C. Open symbols represent experimental data from this study, and closed symbols are data reproduced from ref 8.

with a horizontal, temperature-controlled ATR cell (Specac Inc.). The PMMA/PVP/PS films were deposited on a multiple reflection, trapezoidal zinc selenide ATR crystal (Specac Inc.) with 45° beveled faces. All spectra were collected using a liquid nitrogen-cooled mercury−cadmium−telluride (MCT) detector with 32 scans per spectrum at a resolution of 2 cm^{-1}, where a spectrum was collected every 15 s. FTIR-ATR experiments were conducted at 35 °C (25 °C for PMMA), controlled via a temperature jacket (circulated water bath) on the ATR flow-through cell. The ATR flow-through cell was connected directly to the same vapor sorption apparatus as the QSM. Before each sorption experiment, a background spectrum of the bare ATR crystal was collected, and all subsequent collected spectra were subtracted from this spectrum. Then, a polymer-coated ATR crystal was mounted into the ATR flow-through cell with a Kalrez gasket and the cell was sealed. To begin each sorption experiment, the vapor sorption/ATR combined system was evacuated for at least 2 h prior to the start of each experiment (i.e., pressure transducer reached constant value). Then pure water vapor was charged into the vapor sorption system at a specific vapor pressure and allowed to equilibrate (i.e., the pressure transducer reading was constant). Once steady-state was reached, the valve separating the ATR cell from the rest of the system was opened, allowing pure water vapor to enter the ATR cell in the space (V = 550 μL) above the polymer film (the side opposite the polymer−crystal interface). This was followed by the collection of time-resolved infrared spectra in order to ascertain water in the polymer at a given water vapor activity (i.e., spectra at pseudoequilibrium times were obtained for different water vapor activities to examine water clustering in the polymer). More details regarding the apparatus and experimental procedures can be found elsewhere.[33]

RESULTS

Water Sorption and Water Clustering. Figure 1 shows the sorption isotherms of water in PMMA, PVP, and PS, measured with QSM at 35 °C. The water sorption data were collected over a wide range of water vapor activity (ca. 0−0.82); corresponding water sorption values for each of the glassy polymers studied varied over 3 orders of magnitude.

In Figure 1, the data collected in this study is compared with data collected by Rodríguez et al.[8] It can be seen from Figure 1a and b that the water solubility data collected in this study is in perfect agreement with data from a previous study for water/PMMA, while data collected for water/PVP is lower than that previously reported (ca. 25% variation). Among the three polymers investigated, water solubility was highest in PVP, with concentrations as high as 300 mg_{water}/g_{PVP} at water activities above 0.80. In contrast, water solubility, at the same activity, in PMMA was an order of magnitude lower (ca. 15 mg_{water}/g_{PMMA}), and in PS it was 2 orders of magnitude lower than PVP (ca. 1.5 mg_{water}/g_{PS}). Due to the fact that PVP is a hydrophilic

dx.doi.org/10.1021/jp405388d | J. Phys. Chem. B 2013, 117, 10629−10640

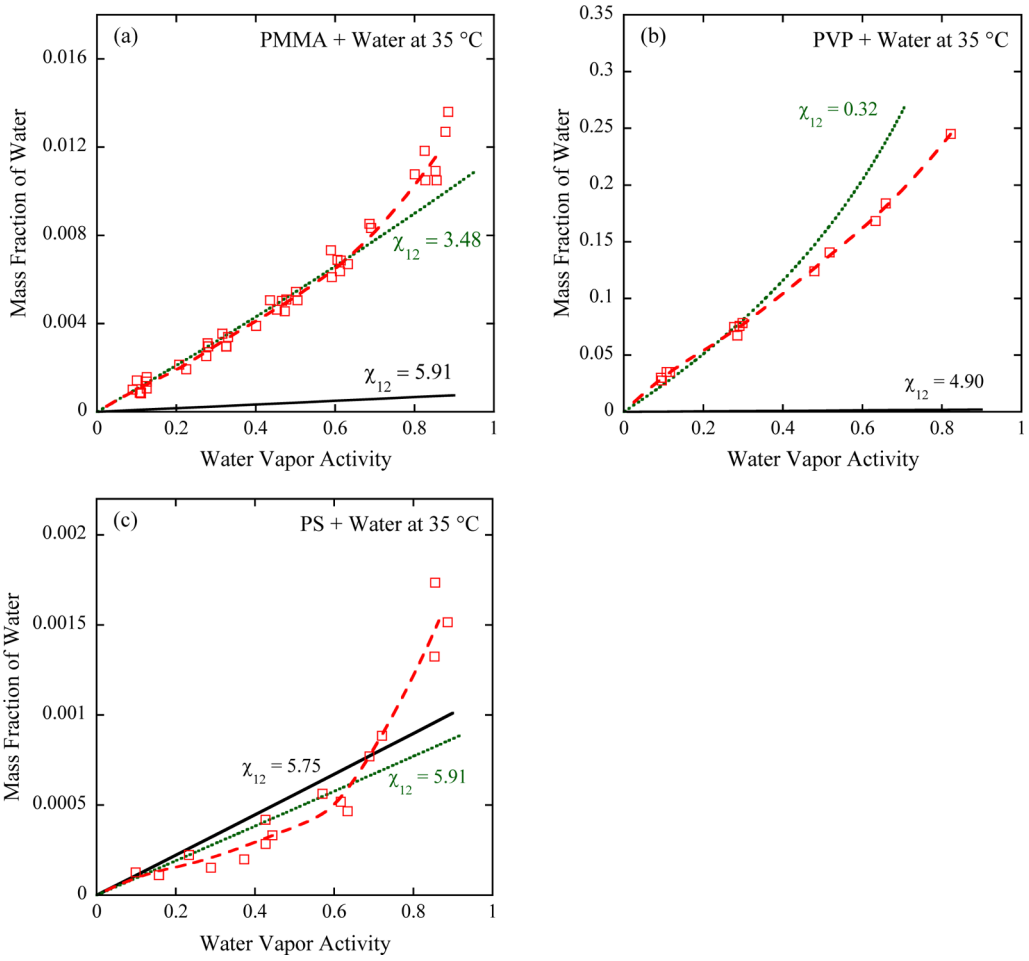

Figure 2. Flory–Huggins model predictions (solid lines) and regressions with fixed (dotted lines) and variable (dashed lines) χ_{12} parameters of water sorption in (a) PMMA, (b) PVP, and (c) PS at 35 °C compared to QSM data collected in this study (open symbols).

polymer (i.e., PVP is soluble in liquid water), it is not surprising that water solubility values in PVP are orders of magnitude higher than those measured for PMMA and PS.

To further elucidate the water solubility and water/polymer interactions, the Flory–Huggins model[34−36] was evaluated in relation to this sorption data. The Flory–Huggins model has been used to correlate phase equilibria of solution mixtures containing polymers, using a single, temperature-dependent interaction parameter, χ_{12}. For a binary polymer–solvent mixture, the activity of phase 1 (in this case water) in phase 2 (in this case PMMA, PVP, or PS) can be represented by the following equation:

$$\ln a_1 = \ln \phi_1(1 - 1/r)(1 - \phi_1) + \chi_{12}(1 - \phi_1)^2 \quad (2)$$

where a_1 and ϕ_1 are the water activity and water volume fraction, respectively, r is the ratio of the polymer molar volume to the solvent molar volume, and χ_{12} is the interaction parameter for the two-component mixture. The interaction parameter can be independently calculated from solubility parameters using the following equation:[37]

$$\chi_{12} = \frac{\upsilon_1[\delta_2 - \delta_1]^2}{RT} \quad (3)$$

where υ_1 is the molar volume of water, δ_1 and δ_2 are the solubility parameters for water and glassy polymer, respectively, T is the temperature of the system, and R is the ideal gas constant in the appropriate units. For example, using the solubility parameters of water (47.9 $MPa^{0.5}$)[38] and PMMA (19.0 $MPa^{0.5}$),[39] a χ_{12} value of 5.91 at 35 °C can be calculated. With the value of χ_{12} calculated independently, the Flory–Huggins is absent of fitting parameters and can be used to predict the solubility of water in PMMA. A similar calculation can be carried out to determine the χ_{12} interaction parameter for water/PVP (δ_2 = 21.6 $MPa^{0.5}$)[40] and water/PS (δ_2= 19.4 $MPa^{0.5}$; average of range in literature).[41] The results of the Flory–Huggins prediction of the sorption isotherm of water in PMMA, PVP, and PS at 35 °C using the calculated interaction parameters from eq 3 are shown in Figure 2.

From Figure 2, it is clear that the Flory–Huggins prediction does not adequately predict the water solubility in PMMA and PVP at 35 °C, where the model underpredicts the experimental data by orders of magnitude (Figure 2a and b). Additionally, the Flory–Huggins model does not adequately predict water solubility in PS at 35 °C, but appears significantly better than water/PMMA and water/PVP. In addition to predicting water solubility with the Flory–Huggins model and a calculated χ_{12} parameter (from eq 3), the χ_{12} parameter can also be determined by regressing the sorption data to the Flory–Huggins model (eq 2), where χ_{12} is the fitting parameter. The results of this analysis for PMMA, PVP, and PS at 35 °C are also shown in Figure 2. When the experimental sorption isotherms are regressed to the Flory–Huggins model with one fixed χ_{12} as the fitting parameter, the model provides a more

dx.doi.org/10.1021/jp405388d | J. Phys. Chem. B 2013, 117, 10629−10640

reasonable representation of water solubility data in all three glassy polymers. With the exception of the water/PS mixture, the regressed χ_{12} for water/PMMA and water/PVP mixtures is quite different than the one obtained from pure component solubility parameters; χ_{12} = 5.91 versus 3.48 for water/PMMA and χ_{12} = 4.90 versus 0.32 for water/PVP. Excellent agreement between the experimental sorption data and the Flory–Huggins model can be achieved if the model is regressed to a variable χ_{12} (i.e., varies as a function of mass fraction of water), where a trend line of this regressed data is also shown in Figure 2. In other words, a regressed variable χ_{12} parameter was determined at each experimental solubility data point in Figure 2 to obtain a concentration-dependent interaction parameter, where the results of this analysis are shown in Figure 3.

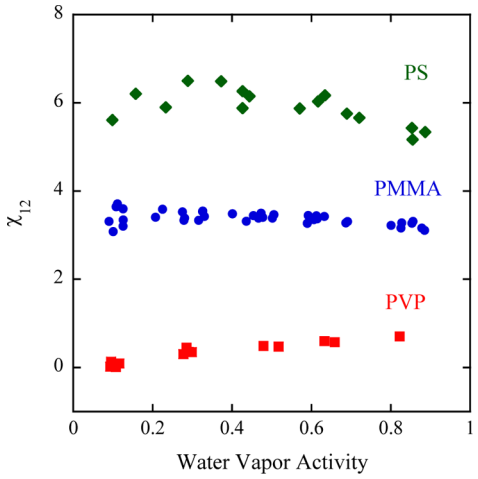

Figure 3. Regressed Flory–Huggins variable χ_{12} parameter for water and PMMA, PVP, and PS at 35 °C as a function of water vapor activity.

As seen from Figure 3, the χ_{12} parameter for each water/glassy polymer mixture is relatively independent of water activity and span from a value of ca. 0.3 for water/PVP to a value of ca. 6 for water/PS. When comparing the χ_{12} parameters obtained from pure component solubility parameters (see Figure 2) and those obtained from a regression of the water sorption isotherms to the Flory–Huggins equation with variable χ_{12} parameters (see Figures 2 and 3), a discrepancy between values obtained for water/PMMA and water/PVP is observed. A value of 5.91 and 4.90 for χ_{12} for water/PMMA and water/PVP, respectively, was calculated from solubility parameters, while values of ca. 3.5 and 0.3 were obtained for water/PMMA and water/PVP, respectively, from the regression. In contrast, the χ_{12} interaction parameter obtained for water/PS from both methods was similar (ca. 5.8). This provides a rationale for the more reasonable prediction of the water solubility data in PS due to the fact that the regressed χ_{12} and χ_{12} obtained from solubility parameters are similar.

The variation in calculated and regressed χ_{12} parameters for water/PMMA and water/PVP can be attributed to the thermodynamic equilibrium framework under which the Flory–Huggins theory is derived. Consequently, the Flory–Huggins theory strictly applies to solutions and mixtures involving rubbery polymers or solvent/polymer mixtures with low glass transition temperatures with respect to experimental temperatures (i.e., polymers in an equilibrium state).[6,8] Alternatively, when one component of the mixture is a glassy polymer and the other component is relatively dilute, equilibrium thermodynamics is no longer valid due to the nonequilibrium nature of the glassy polymer (i.e., time-dependent volume relaxation).[9] Without directly accounting for the departure from equilibrium,[42,43] the Flory–Huggins theory fails to predict water solubility in a polymer in a nonequilibrium, glassy state. Note that there is little difference between the Hildebrand water parameter (48.0 $MPa^{1/2}$) and the Hansen water parameter (47.8 $MPa^{1/2}$), where the latter accounts for hydrogen-bonding interactions.[38] Therefore, these small differences among different solubility parameters would have little impact on the interaction parameter, χ_{12}, calculation in eq 3, which is in the Flory–Huggins model in eq 2. Therefore, the primary factor for the significant difference between the Flory–Huggins theory and water solubility data appears to be the nonequilibrium state of the glassy polymer.

Qualitatively, a large value of χ_{12} indicates unfavorable interactions between the penetrant and polymer, while values close to zero indicate strong interactions between the two components of the mixture. Although the Flory–Huggins model is typically used for solute/polymer or polymer solution mixtures in an equilibrium state, the χ_{12} parameter determined from regressing the solubility data coincides with the trend in QSM water solubility data, where water solubility increases from PS < PMMA < PVP. The mixture with the lowest water solubility, water/PS, has the highest χ_{12} parameter, while the mixture with the highest water solubility, water/PVP, has a χ_{12} value close to zero over the entire water activity range. The χ_{12} parameters obtained for both water/PMMA and water/PVP in this study (Figure 3) match well with those reported by Rodríguez et al.[8]

Each sorption isotherm in Figure 1 exhibits a linear relationship between water concentration and external water vapor pressure at lower pressures (below 3 kPa), while at higher external water vapor pressures all three isotherms show an upturn. There are often three physical explanations offered for this deviation from linearity at higher water vapor activities: (1) polymer dilation (or swelling), (2) plasticization of the polymer, and/or (3) clustering, or self-association due to hydrogen bonding, of water molecules.[8] To determine if any of the water/glassy polymer mixtures go through a plasticization process during the water sorption experiment, the Flory–Fox equation was employed to calculate the suppression in glass transition temperature (T_g) of each polymer. The Flory–Fox equation is shown by the following:[44]

$$\frac{1}{T_{g,m}} = \frac{w_w}{T_{g,w}} + \frac{w_p}{T_{g,p}} \tag{4}$$

where w_w and w_p are the weight fractions of water and polymer, respectively, and $T_{g,m}$, $T_{g,w}$, and $T_{g,p}$ are the glass transition temperatures of the mixture, water, and polymer, respectively. $T_{g,w}$ is equal to −135 °C.[8,45−47] With known weight fractions of water in the polymers (see data in Figure 1) and glass transition temperatures of the dry polymer (T_g = 119, 181, and 101 °C for PMMA, PVP, and PS, respectively),[8,30] a calculation of the glass transition temperature of the mixture can be determined. Using the Flory–Fox equation, the glass transition temperature of each water/glassy mixture was calculated at various water vapor activities. From this analysis, it was determined that the PMMA and PS remain glassy ($T_{g,m}$ = 111 and 100 °C at a water vapor activity of ca. 0.80 for water/PMMA and water/PS, respectively), while for PVP, a T_g of 50 and 18 °C were

dx.doi.org/10.1021/jp405388d | J. Phys. Chem. B 2013, 117, 10629−10640

determined at a water vapor activity of ca. 0.60 and 0.80, respectively. It is clear from this calculation that enough water is sorbed into PVP at a high water vapor activity to plasticize the polymer, whereby the T_g of the material is suppressed below the experimental temperature (35 °C). Therefore, the water/PMMA and water/PS mixtures are in a nonequilibrium state throughout for the entire mixture composition (water activity range), while the water/PVP mixture is in a nonequilibrum state over a significant portion of the mixture composition range, but is in an equilibrium state (becomes a rubber due to plasticization)[6,8] at high vapor activities (confirmed by the Flory–Fox equation). Previous research has shown that when the nonequilibrium state of the glassy polymer is considered via nonequilibrium thermodynamics (e.g, nonequilibrium lattice fluid (NELF) model and nonequilibrium statistical associating fluid theory (NE-SAFT)), accurate predictions of water solubility in glassy polymers can be obtained over a wide range of water vapor activity and temperature.[25,48]

While this calculation may explain the upturn in the water sorption isotherm at higher water activities for PVP, this does not provide a rationale for the upturn in the sorption data for PMMA and PS. Another phenomenon to consider is water clustering in these glassy polymers. As previously mentioned, the Zimm–Lundberg clustering function has been frequently used to evaluate the extent of clustering of sorbed molecules inside a polymer. The major advantage of the Zimm–Lundberg clustering function is that it can be calculated directly from water solubility measurements (i.e., water sorption isotherm). According to the Zimm–Lundberg theory, clustering of water in a polymer can be mathematically represented by the clustering function shown below:[8]

$$\frac{G_{11}}{v_1} = -(1-\phi_1)\left[\frac{\partial(a_1/\phi_1)}{\partial a_1}\right]_{T,P} - 1 \tag{5}$$

where G_{11}/v_1 is the clustering function and a_1 and ϕ_1 are the water vapor activity and volume fraction, respectively. When values of the clustering function are below a value of −1, water molecules exclude their volume to adjacent molecules and no clustering occurs.[49] The extent to which clustering occurs within the polymer can be represented by how much $G_{11}/v_{11} > -1$,[23] and this clustering function can be determined from water sorption data of absorbed water volume fraction and water vapor activity. Furthermore, the average number of water molecules in a cluster, or the mean cluster size (MCS), can be calculated from the following equation.

$$\text{MCS} = 1 + \frac{\phi_1 G_{11}}{v_{11}} \tag{6}$$

Subsequently, the mean cluster size ($1 + \phi_1 G_{11}/v_1$ vs a_1) was calculated from the QSM sorption data (Figure 1), and the results of this analysis are shown in Figure 4.

As seen from Figure 4, the Zimm–Lundberg function predicts a MCS of water in PMMA that slightly increases with increasing activity with water as monomers at low activity and growing in size to dimers or a mixture of monomers and dimers at higher activity. These results are in adequate agreement with those previously obtained by Rodríguez et al.[8] Similarly, the MCS for water in PS initially indicates monomers at low water activities, but shows the presence of dimers and trimers at higher water vapor activities. In contrast, the MCS for water in PVP predicts only monomers over the entire activity range.

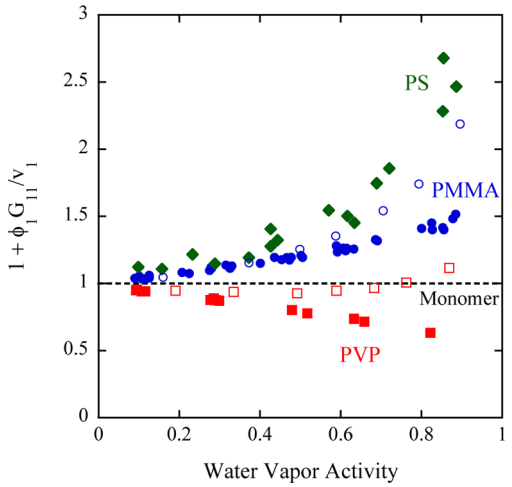

Figure 4. MCS of water in PMMA, PVP, and PS at 35 °C as function of water vapor activity as determined by the Zimm–Lundberg clustering function. MCS = 1 represents a monomer of water, whereas MCS = 2 and 3 represent dimer and trimer, respectively. Filled symbols represent calculation from experimental data in this work, while open symbols represent calculations from ref 8.

Again, these results are in adequate agreement with previous work by Rodríguez et al.[8] The slight differences in the calculated MCS from this work and previous work[8] may be due to differences in the regression techniques used. While the Zimm–Lundberg clustering analysis can provide a prediction of water clustering in a polymer from solubility data, the model was developed under the framework of thermodynamic equilibrium, similar to the Flory–Huggins model. From our analysis of the glass transition temperature for these water/glassy polymer mixtures, where it was determined that these mixtures are predominantly in a nonequilibrium state at the experimental temperature, it is clear that the thermodynamic equilibrium assumption may not describe these mixtures adequately. Therefore, a direct measurement of water clustering in these polymers in their nonequilibrium state would be of interest. To provide a direct measurement of water clustering in these glassy polymers during the water sorption experiment, in situ FTIR-ATR spectroscopy was employed, where O–H bonds for different populations of water have distinct infrared bands and can be individually distinguished.

Figure 5 shows the mid-infrared spectra of the O–H stretching region for water in PMMA, PVP, and PS after the polymers were exposed to various water vapor activities.

As seen in Figure 5a, there are three predominant infrared bands present in the O–H stretching region of the mid-infrared spectra in PMMA. The additional band located at ca. 3440 cm^{-1} is associated with the carbonyl (C═O) stretching overtone of the PMMA (shown by dashed arrow in Figure 5a).[50] Two predominant bands located at ca. 3550 and 3615 cm^{-1} can be attributed to the O–H stretching of the water dimer and "free" O–H stretching, respectively.[51−54] These peaks are typically found at higher wavenumbers, but may be shifted slightly due to a different environment (i.e., in PMMA). Other investigators have suggested that these two infrared bands are associated with the symmetric and asymmetric, respectively, of the O–H stretching of a water molecule hydrogen bound to two C═O groups of the polymer.[55,56] Recent work by Davis and Elabd[48] showed that when the intensity of these two infrared bands are plotted against each

dx.doi.org/10.1021/jp405388d | J. Phys. Chem. B 2013, 117, 10629−10640

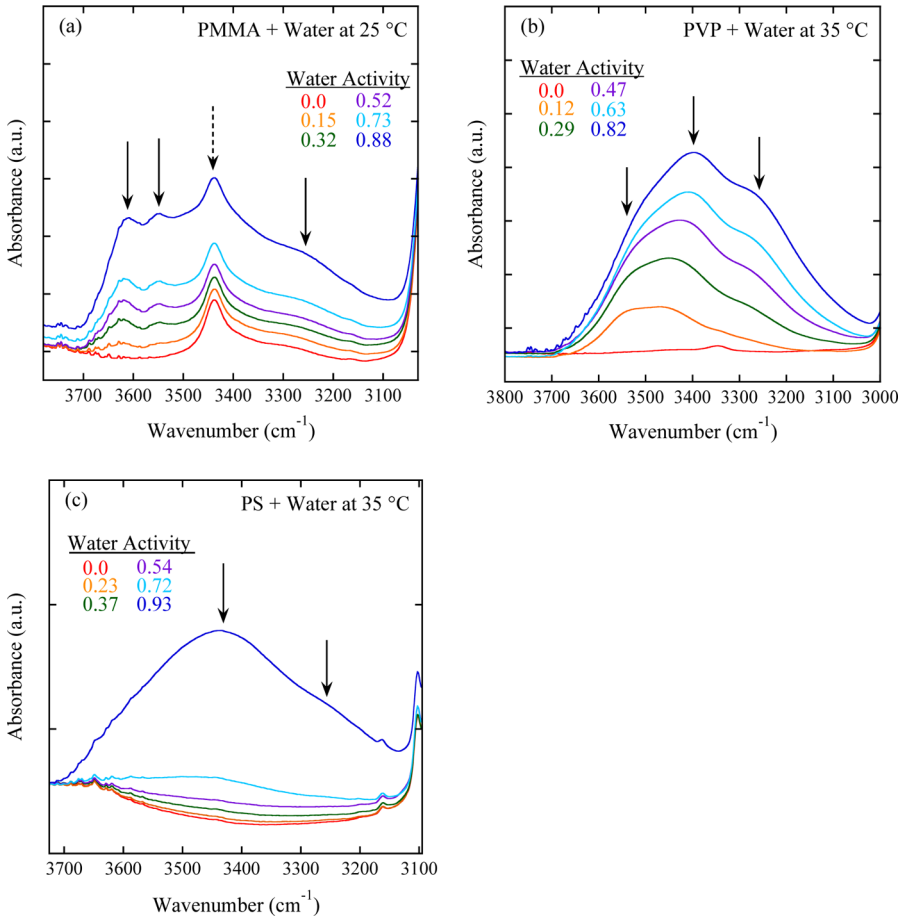

Figure 5. FTIR-ATR spectra of the O−H stretching region of water in (a) PMMA (25 °C), PVP (35 °C), and PS (35 °C) after exposure to several different water vapor activities (numbers on graph).

other, there is a deviation from linearity at higher water vapor activities, indicating that these two bands do not represent the same population of water. In other words, at lower water vapor activities, where a linear relationship is observed between these two IR bands, both IR signatures are representative of the same species of water (i.e., dimer). At higher water vapor activities, the deviation from linearity between the two bands suggests that the "free" O−H stretching band at the highest wavenumber is no longer representative of a single cluster size, but corresponds to both the water dimer and higher-sized water clusters (e.g., trimer, hexamers).[57] This physical picture of water clustering in PMMA is confirmed by the presence of a broader infrared band located between ca. 3100 and 3350 cm^{-1} (associated with larger, hydrogen-bound water clusters),[51] which begins to increase in intensity, but becomes clearly evident at water activities at and above 0.73.

As seen from Figure 5b, water clustering in PVP is significantly different than those in PMMA, where three IR bands can be observed at all water activities. The first band, located at the highest wavenumber (ca. 3550 cm^{-1}), can again be assigned to the water dimer. The two IR bands located directly to the right (at ca. 3450 cm^{-1} and ca. 3250 cm^{-1}) of the water dimer band, can be attributed to self-associated, hydrogen-bonded water clusters, where the IR band at the lower wavenumber can be assigned to water clusters with the highest strength of self-association.[27] As seen from Figure 5b, the IR band associated with the water dimer transitions into a shoulder at higher wavenumbers, indicating that this population of water may decrease as a function of water activity (but this is highly dependent on the absorption coefficients of the different bands at different wavenumbers), indicating that water may predominately exist as larger self-associated, hydrogen-bonded water clusters in PVP (also seen by a significant increase in IR intensity of bands corresponding to associated water clusters). Similarly, the infrared spectra for water in PS (Figure 5c) indicate that water primarily exists as larger self-associated clusters over the entire water activity range (shown by two predominant IR bands at ca. 3450 cm^{-1} and ca. 3275 cm^{-1}). The water clustering shown by the infrared spectra for both PVP and PS are different than those shown for PMMA, where self-associated water clusters are only present at higher water vapor activities (above ca. 0.50).

The results obtained from FTIR-ATR spectroscopy for the water cluster sizes in these glassy polymers appear to contradict the results obtained from the Zimm−Lundberg clustering analysis. Specifically, direct measurements from FTIR-ATR spectroscopy show that highly self-associated, hydrogen-bound water clusters are the prevalent population of water in PVP, where the Zimm−Lundberg model predicts only nonassociated, water monomers over the entire activity range. Similarly, the Zimm-Lundberg analysis provides a contradictory physical picture for the water clustering in PMMA, where monomers are predicted at lower activities (i.e., below ca. 0.50) and dimers are predicted at higher water activities. Direct measurements from FTIR-ATR spectroscopy show the presence of water dimers at lower water vapor activities, but no signature IR band

dx.doi.org/10.1021/jp405388d | J. Phys. Chem. B 2013, 117, 10629−10640

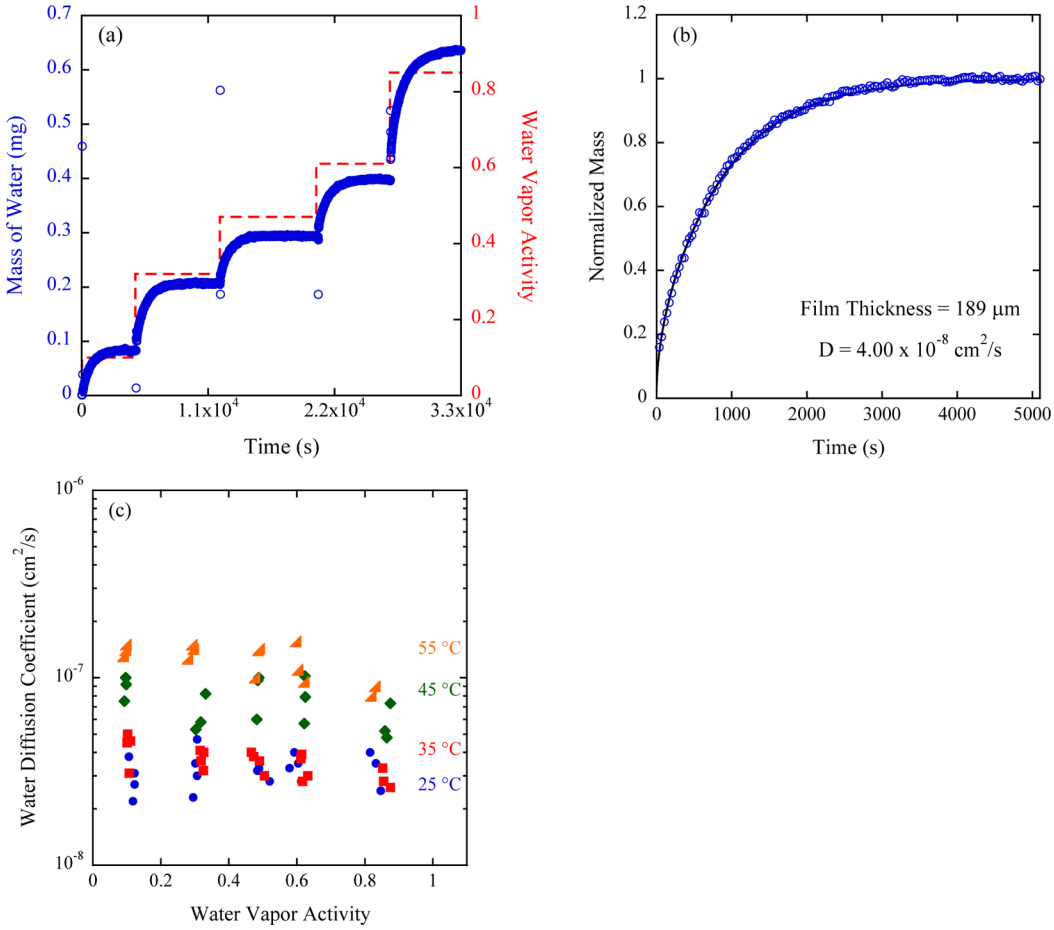

Figure 6. QSM data: (a) multiple water sorption kinetic curves in PMMA at 35 °C in response to multiple different external water vapor activities (step changes) over a broad range of 0 to 0.85. Outlier data points are a result of the buoyancy response of the spring in response to sudden step changes in vapor activity. (b) Water sorption kinetics in PMMA at 35 °C in response to an external differential water vapor activity step change of 0.11 to 0.33. The solid black line represents a regression of the experimental data to eq 1,[32] where the diffusion coefficient, *D*, was the only adjustable parameter. (c) Water diffusion coefficients in PMMA over a wide range of water activities at 25, 35, 45, and 55 °C.

associated with the water monomer was observed in the spectra at any activity. Furthermore, IR spectroscopy indicates the presence of water clusters at higher water vapor activities (above ca. 0.50), where the Zimm–Lundberg analysis only indicates the presence of water dimers in PMMA at these elevated activities. For PS, a similar contradictory physical picture for water clustering was observed between the direct IR measurements and Zimm–Lundberg analysis, where monomers and dimers are prevalent at most activities from the Zimm–Lundberg analysis, even though direct, molecular-level measurements show the presence of larger self-associated water clusters throughout the entire activity range.

The results of this analysis (Figures 4 and 5) indicate that the Zimm–Lundberg clustering function may only be used to compliment IR spectroscopy data, but may not be sufficient as the sole analysis to determine the extent of penetrant clustering in a polymer. The contradictory picture provided from the Zimm–Lundberg clustering analysis may be attributed the equilibrium framework under which the theory was derived, which cannot adequately describe the water/glassy polymer mixtures in this study, which are in a nonequilibrium state. However, in the future, it would be of interest to compare the Zimm–Lundberg approach to infrared data for water/polymer mixtures in an equilibrium state.

Water Sorption Kinetics and Water Clustering. The impact of water clustering on sorption kinetics (diffusivity), as well as sorption, was investigated. Figure 6a shows water sorption kinetics in PMMA measured by QSM. Specifically, multiple sorption kinetic curves are shown in response to multiple differential changes in external water vapor pressure (steps in water activity ranging from 0.10 to 0.20 over a larger range of 0–0.85).

Figure 6b shows that diffusion of water in PMMA is Fickian as indicated by an adequate regression to eq 1. Non-Fickian or two-stage sorption kinetic behavior for water in PMMA has been observed previously due to the nonequilibrium nature of the water/PMMA mixture; however, the data can appear Fickian (as in Figure 6b) if the time scale of each sorption step is fast in reference to the polymer film thickness. In this study, all polymer films were thick in relation to time scale of experiment to capture only Fickian kinetics, where the diffusivity was determined from a regression of the water uptake curves to a solution of Fick's second law (eq 1).[32] An example is shown in Figure 6b, where the diffusion coefficient, *D*, was the only adjustable parameter. A diffusion coefficient of 4.00×10^{-8} cm^2/s was obtained from the regression and is in excellent agreement with the experimental data. The diffusion coefficients calculated from QSM fall within the range of values reported in literature,[58−61] where small variations between

dx.doi.org/10.1021/jp405388d | J. Phys. Chem. B 2013, 117, 10629−10640

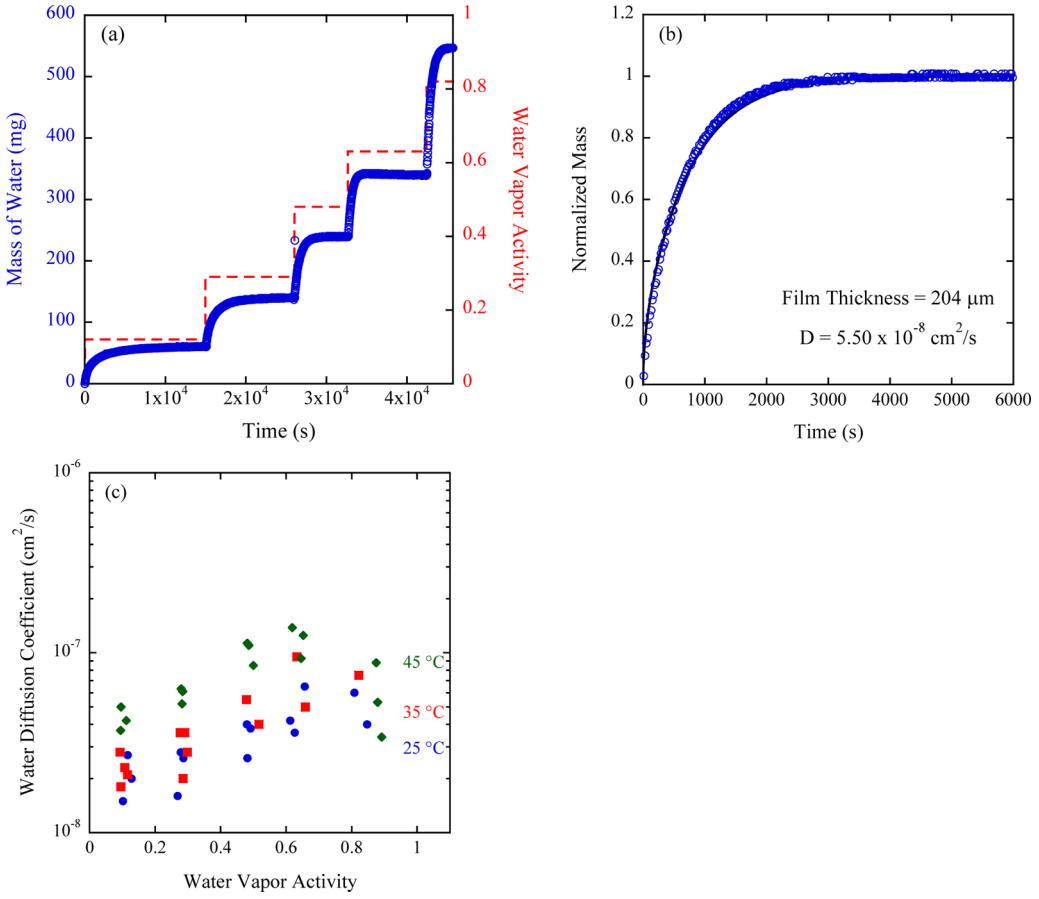

Figure 7. QSM data: (a) multiple water sorption kinetic curves in PVP at 35 °C in response to multiple different external water vapor activities (step changes) over a broad range of 0 to 0.82. (b) Water sorption kinetics in PVP at 35 °C in response to an external differential water vapor activity step change of 0.29 to 0.48. The solid black line represents a regression of the experimental data to eq 1,[32] where the diffusion coefficient, *D*, was the only adjustable parameter. (c) Water diffusion coefficients in PVP over a wide range of water activities at 25 (blue circles), 35 (red squares), and 45 °C (green diamonds).

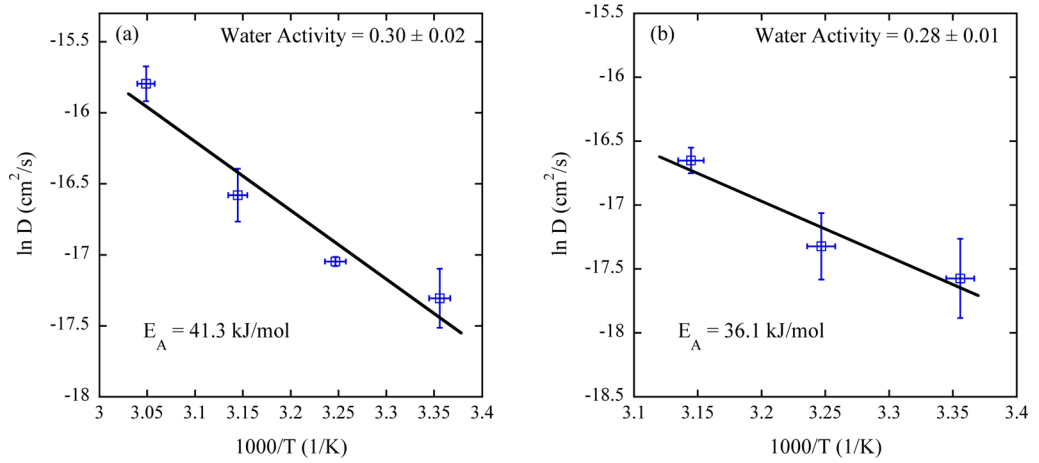

Figure 8. Activation energy for diffusion for water in (a) PMMA and (b) PVP at a water vapor activity of ca. 0.30.

values may be due to different processing conditions of the glassy polymers (i.e., thermal history plays an important role in final nonequilibrium structure of the polymer). Figure 6c shows all the diffusion coefficients calculated at 25, 35, 45, and 55 °C over the entire water vapor activity range investigated, where the values increase with increasing temperature and slightly decrease with increasing water vapor activity. This decrease in water diffusivity with increasing water vapor activity has often been attributed the self-association of water (formation of water clusters),[62−64] where water increases in size with increasing activity and therefore its diffusivity decreases. This physical picture was verified spectroscopically in this study (see Figure 5a).

Figure 7a shows water sorption kinetics in PVP measured by QSM. Specifically, multiple sorption kinetic curves are shown in response to multiple differential changes in external water vapor

dx.doi.org/10.1021/jp405388d | J. Phys. Chem. B 2013, 117, 10629−10640

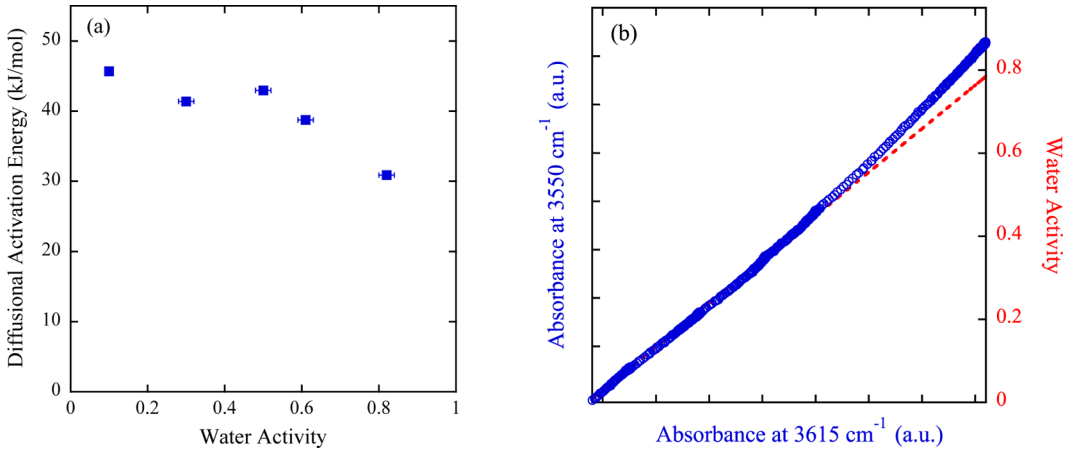

Figure 9. (a) Activation energy for diffusion of water in PMMA as a function of water vapor activity. (b) Integrated, time-resolved water O−H stretching infrared absorbance (open circles) associated with the free O−H and dimer hydrogen-bonded O−H plotted against each other over the entire length of a sorption experiment. Dashed line corresponds to 45° line.

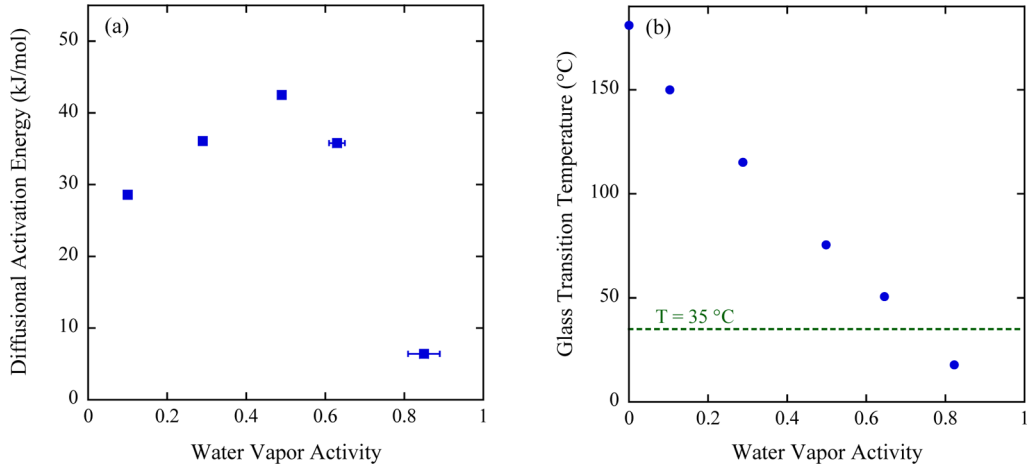

Figure 10. (a) Activation energy for diffusion of water in PVP as a function of water vapor activity. (b) Glass transition temperature of the water/PVP mixture plotted versus water vapor activity. Dashed line represents an experimental temperature of 35 °C.

pressure (steps in water activity ranging from 0.10 to 0.20 over a larger range of 0 to 0.82).

Figure 7b shows sorption kinetics of water in PMMA in response to single differential change in water vapor activity of 0.29 to 0.48, where excellent agreement between the model and experimental data was observed again and a water diffusion coefficient of 5.50×10^{-8} cm^2/s was determined. The diffusion coefficients obtained from this analysis fall within the range of those previously reported in literature.[8] Figure 7c shows all the diffusion coefficients calculated at 25, 35, and 45 °C over the entire water vapor activity range investigated, where the values increase with increasing temperature and exhibit a parabolic shape (increasing then decreasing) with increasing water vapor activity. The observed parabolic behavior of the water diffusivity versus water vapor activity is suggestive of water clustering increasing with activity. In other words, diffusivity increases with increasing water concentration due to an increase in the free volume of the mixture (water sorbs more in PVP than PMMA and PS), but then begins to decrease due to the larger size of the diffusant (water cluster size increases with increasing activity). The plasticization of the PVP film with increasing water content may also play a role in this behavior. Furthermore, it is clear from Figure 7c that the diffusion coefficient of water in PVP is highly concentration dependent, and the application of single, concentration-averaged diffusion coefficient may not be a sufficient representation of the water sorption kinetics of the water/PVP mixture.

With water diffusivities values obtained at different temperatures, an Arrhenius activation energy for diffusion at each water vapor activity of interest can be obtained. An example of this analysis is shown in Figure 8 for PMMA and PVP at a water vapor activity of ca. 0.30.

Figure 8 shows a semilog plot of diffusivity versus inverse temperature with a regression to the Arrhenius equation to determine the activation energy for diffusion. As seen in Figure 8, the activation energy of diffusion of water in PMMA is higher than that of water in PVP at the same water vapor activity. Physically this means that more energy is required for water to make diffusional jumps in PMMA than in PVP at a water vapor activity of 0.30.

Figure 9 shows the activation energies for diffusion as a function of water vapor activity for PMMA obtained by using the same analysis shown in Figure 8 at different water activities.

For water/PMMA, the activation energy for diffusion decreases from a value of ca. 45 kJ/mol to ca. 30 kJ/mol with increasing water vapor activity from 0.10 to 0.83. It is interesting to note how these activation energies for diffusion correlate with the energy required to break the hydrogen bond

dx.doi.org/10.1021/jp405388d | J. Phys. Chem. B 2013, 117, 10629−10640

of the water dimer. Recent investigators report a dissociation energy of the hydrogen bond of the water dimer species to be ca. 15 kJ/mol.[65] As seen from Figure 9a, the activation energy for diffusion remains above a value of ca. 40 kJ/mol for water vapor activities below ca. 0.50, corresponding to a higher energy than twice that of the energy required to dissociate a single hydrogen bond. This region (<0.5 activity) coincides with the presence of dimers (one hydrogen bond) in PMMA as evidenced by IR spectroscopy (see Figure 5a). Interestingly, a decrease in diffusional activation energy below ca. 40 kJ/mol occurs at a water vapor activity above ca. 0.5, which coincides with the appearance of larger water clusters in PMMA observed with IR spectroscopy (see Figure 5a).

This phenomenon is further highlighted in Figure 9b, which shows a plot of the hydrogen-bonded O−H dimer band at 3550 cm^{-1} versus the free O−H band at 3615 cm^{-1} over the entire water sorption experiment. Below a water activity of ca. 0.5, a linear relationship between the increase of these two bands can be observed. This linear relationship suggests that these two IR bands are representative of the same species of water, the water dimer. Additionally, at water activities above ca. 0.50, a deviation from linearity is observed in Figure 9b. This deviation from linearity suggests that the two IR bands are no longer representative of the same species. In other words, above a water vapor activity of 0.50, large clusters of water are also present in PMMA, and therefore the free O−H band at 3615 cm^{-1} represents not only the water dimer, but also higher water cluster sizes. Furthermore, this deviation in linearity, indicating the presence of larger, hydrogen-bonded water clusters, coincides with the drop in activation energy for diffusion below that of a value of ca. 40 kJ/mol. Additionally, this analysis was performed on the water/PVP mixture, where the results of this analysis are shown in Figure 10.

Contrastingly, the activation energy for diffusion for water in PVP (Figure 10a) increases from ca. 30 kJ/mol to ca. 42 kJ/mol, where it peaks at a water activity of 0.50, and then decreases to below 10 kJ/mol at a high activity (i.e., parabolic). For the water in PVP case, similar arguments to that of the water/PMMA mixture are not appropriate, since the PVP sorbs significantly more water (not in the semidilute region) than PMMA and even plasticizes at high water vapor activities. The plasticization of PVP by water is shown in Figure 10b, where the glass transition temperature of the water/PVP mixture was determined using the Flory−Fox equation.[44] The significant decrease in the diffusional activation energy at an activity > 0.8 is clearly due to the plasticization of PVP, where the diffusional energy barrier for water is significantly reduced when PVP undergoes this glass−rubber transition.

CONCLUSIONS

In this study, the solubility of water vapor in PMMA, PVP, and PS was measured using quartz spring microbalance (QSM) at a number of experimental temperatures and over a wide range of water vapor activity. The Flory−Huggins theory was employed to predict the water sorption isotherms in these three nonequilibrium, glassy polymers, where model predictions and experimental data did not agree, where this difference can be attributed to the equilibrium framework from which the Flory−Huggins theory is derived. Furthermore, using the water/glassy polymer equilibrium data, a calculation of the extent of clustering in the mixture was determined by the Zimm−Lundberg clustering function, where contrasting physical pictures between the calculated mean cluster size and direct, molecular-level measurements (FTIR-ATR spectroscopy) was observed. Again, this deviation between model predictions and direct infrared measurements may be due to the thermodynamic equilibrium framework with which the clustering model is derived, where the glassy polymers in this study are in a constant, nonequilibrium state. These spectroscopic results indicated that great caution must be taken when using the Zimm−Lundberg analysis as the sole analysis method to describe the extent of water clustering in glassy polymers. Furthermore, a correlation between the activation energy of diffusion and water clustering were observed for water/PMMA and water/PVP. These results provide unique insight into the impact of water clustering on sorption and diffusion in glassy polymers.

AUTHOR INFORMATION

Corresponding Author

*E-mail: elabd@drexel.edu.

Notes

The authors declare no competing financial interest.

ACKNOWLEDGMENTS

The authors acknowledge the financial support of the National Science Foundation (CAREER 0644593).

REFERENCES

(1) Langer, R. S.; Peppas, N. A. *Biomaterials* **1981**, *2*, 201−214.
(2) Cath, T. Y.; Childress, A. E.; Elimelech, M. *J. Membr. Sci.* **2006**, *281*, 70−87.
(3) Geise, G. M.; Lee, H.-S.; Miller, D. J.; Freeman, B. D.; McGrath, J. E.; Paul, D. R. *J. Polym. Sci., Part B: Polym. Phys.* **2010**, *48*, 1685−1718.
(4) Mauritz, K. A.; Moore, R. B. *Chem. Rev.* **2004**, *104*, 4535−4585.
(5) Auras, R.; Harte, B.; Selke, S. *Macromol. Biosci.* **2004**, *4*, 835−864.
(6) Hancock, B. C.; Zografi, G. *Pharm. Res.* **1993**, *10*, 1262−1267.
(7) Arce, A.; Fornasiero, F.; Rodríguez, O.; Radke, C. J.; Prausnitz, J. M. *Phys. Chem. Chem. Phys.* **2004**, *6*, 103−108.
(8) Rodríguez, O.; Fornasiero, F.; Arce, A.; Radke, C. J.; Prausnitz, J. M. *Polymer* **2003**, *44*, 6323−6333.
(9) Frisch, H. L. *Polym. Eng. Sci.* **1980**, *20*, 2−13.
(10) Del Nobile, M. A.; Mensitieri, G.; Netti, P. A.; Nicolais, L. *Chem. Eng. Sci.* **1994**, *49*, 633−644.
(11) Connelly, R. W.; McCoy, N. R.; Koros, W. J.; Hopfenberg, H. B.; Stewart, M. E. *J. Appl. Polym. Sci.* **1987**, *34*, 703−719.
(12) Vrentas, J. S.; Jarzebski, C. M.; Duda, J. L. *AIChE J.* **1975**, *21*, 894−901.
(13) Berens, A. R.; Hopfenberg, H. B. *Polymer* **1978**, *19*, 489−496.
(14) Zimm, B. H. *J. Chem. Phys.* **1953**, *21*, 934−935.
(15) Zimm, B. H.; Lundberg, J. L. *J. Chem. Phys.* **1956**, *60*, 425−428.
(16) Cornejo-Bravo, J. M.; Siegel, R. A. *Biomaterials* **1996**, *17*, 1187−1193.
(17) Beck, M. I.; Tomka, I. *J. Macromol. Sci., Part B: Phys.* **1997**, *36*, 19−39.
(18) Detallante, V.; Langevin, D.; Chappey, C.; Metayer, M.; Mercier, R.; Pineri, M. *J. Membr. Sci.* **2001**, *190*, 227−241.
(19) Kilburn, D.; Claude, J.; Mezzenga, R.; Dlubek, G.; Alam, A.; Ubbink, J. *J. Phys. Chem. B* **2004**, *108*, 12436−12441.
(20) Roussenova, M.; Murith, M.; Alam, A.; Ubbink, J. *Biomacromolecules* **2010**, *11*, 3237−3247.
(21) Weinmüller, C.; Langel, C.; Fornasiero, F.; Radke, C. J.; Prausnitz, J. M. *J. Biomed. Mater. Res. A* **2006**, *77*, 230−241.
(22) Williams, J. L.; Hopfenberg, H. B.; Stannett, V. *J. Macromol. Sci., Part B: Phys.* **1969**, *3*, 711−725.
(23) Du, A.; Koo, D.; Theryo, G.; Hillmyer, M. A.; Cairncross, R. A. *J. Membr. Sci.* **2012**, *396*, 50−56.
(24) Rickles, R. N. *Ind. Eng. Chem.* **1966**, *58*, 19−35.

(25) Davis, E. M.; Minelli, M.; Giancinti Baschetti, M.; Sarti, G. C.; Elabd, Y. A. *Macromolecules* **2012**, *45*, 7486−7494.
(26) Metz, S. J.; van de Ven, W. J. C.; Mulder, M. H. V.; Wessling, M. *J. Membr. Sci.* **2005**, *266*, 51−61.
(27) Sammon, C.; Mura, C.; Yarwood, J.; Everall, N.; Swart, R.; Hodge, D. *J. Phys. Chem. B* **1998**, *102*, 3402−3411.
(28) Pereira, M. R.; Yarwood, J. *J. Chem. Soc., Faraday Trans.* **1996**, *92*, 2731−2735.
(29) Wang, M.; Wu, P.; Sengupta, S. S.; Chadhary, B. I.; Cogen, J. M.; Li, B. *Ind. Eng. Chem. Res.* **2011**, *50*, 6447−6454.
(30) Aras, L.; Richardson, M. J. *Polymer* **1989**, *30*, 2246−2252.
(31) Elabd, Y. A.; Barbari, T. A. *AIChE J.* **2001**, *47*, 1255−1262.
(32) Crank, J. *Mathematics of Diffusion*, 2nd ed.; Wiley: New York, 2003.
(33) Hallinan, D. T., Jr.; Elabd, Y. A. *J. Phys. Chem. B* **2009**, *113*, 4257−4266.
(34) Flory, P. J. *Principles of Polymer Chemistry*; Cornell University Press: London, 1953.
(35) Flory, P. J. *J. Chem. Phys.* **1941**, *9*, 660−661.
(36) Huggins, M. L. *J. Chem. Phys.* **1941**, *9*, 440.
(37) Fan, K.; Niu, L.; Li, J.; Feng, R.; Qu, R.; Liu, T.; Song, J. *Soft Matter* **2013**, *9*, 3057−3062.
(38) Grulke, E. A. Solubility Parameter Values. In *Polymer Handbook*, 4th ed.; Brandrup, J., Immergut, E. H., Grulke, E. A., Eds.; Wiley-Interscience: Hoboken, NJ, 1999; Vol. *2*; p 694.
(39) Vandenburg, H. J.; Clifford, A. A.; Bartle, K. D.; Carlson, R. E.; Carroll, J.; Newton, I. D. *Analyst* **1999**, *124*, 1707−1710.
(40) Forster, A.; Hempenstall, J.; Tucker, I.; Rades, T. *Int. J. Pharm.* **2001**, *226*, 147−161.
(41) DiPaola-Baranyi, G.; Guillet, J. E. *Macromolecules* **1978**, *11*, 228−235.
(42) Doghieri, F.; Sarti, G. C. *Macromolecules* **1996**, *29*, 7885−7896.
(43) Carla, V.; Wang, K.; Hussain, Y.; Efimenko, K.; Genzer, J.; Grant, C.; Sarti, G. C.; Carbonell, R. G.; Doghieri, F. *Macromolecules* **2005**, *38*, 10299−10313.
(44) Fox, T. G. *Bull. Am. Phys. Soc.* **1956**, *1*, 123.
(45) Schult, K. A.; Paul, D. R. *J. Polym. Sci., Part B: Polym. Phys.* **1996**, *34*, 2805−2817.
(46) Buera, M. D.; Levi, G.; Karel, M. *Biotechnol. Prog.* **1992**, *8*, 144−148.
(47) Oksanen, C. A.; Zografi, G. *Pharm. Res.* **1990**, *7*, 654−657.
(48) Davis, E. M.; Elabd, Y. A. *Ind. Eng. Chem. Res.* **2013**, DOI: 10.1021/ie401713h.
(49) Starkweather, H. W. *J. Polym. Sci., Part B: Polym. Lett.* **1963**, *1*, 133−138.
(50) Willis, H. A.; Zichy, V. J. I.; Hendra, P. J. *Polymer* **1969**, *10*, 737−746.
(51) Scatena, L. F.; Brown, M. G.; Richmond, G. L. *Science* **2001**, *292*, 908−912.
(52) Du, Q.; Superfine, R.; Freysz, E.; Shen, Y. R. *Phys. Rev. Lett.* **1993**, *70*, 2313−2316.
(53) Buck, U.; Huisken, F. *Chem. Rev.* **2000**, *100*, 3863−3890.
(54) Paul, J. B.; Collier, C. P.; Saykally, R. J.; Scherer, J. J.; O'Keefe, A. *J. Phys. Chem. A* **1997**, *101*, 5211−5214.
(55) Iwamoto, R.; Matsuda, T. *Anal. Chem.* **2007**, *79*, 3455−3461.
(56) Iwamoto, R.; Matsuda, T. *J. Polym. Sci., Part B: Polym. Phys.* **2005**, *43*, 777−785.
(57) Pérez, C.; Muckle, M. T.; Zaleski, D. P.; Seifert, N. A.; Temelso, B.; Shields, G. C.; Kisiel, Z.; Pate, B. H. *Science* **2012**, *336*, 897−901.
(58) Roussis, P. P. *J. Membr. Sci.* **1983**, *15*, 141−155.
(59) Barrie, J. A.; Machin, D. *Trans. Faraday Soc.* **1971**, *67*, 244−256.
(60) Bueche, F. *J. Polym. Sci.* **1954**, *14*, 414−416.
(61) Hsu, W. P.; Li, R. J.; Myerson, A. S.; Kwei, T. K. *Polymer* **1993**, *34*, 597−603.
(62) Polishchuk, A. Y.; Zaikov, G. E. *Multicomponent Transport in Polymer Systems for Controlled Release*; Gordon and Breach Science: Amsterdam, 1997.
(63) Wellons, J. D.; Stannett, V. *J. Polym. Sci., Part A-1: Polym. Chem.* **1966**, *4*, 593−602.
(64) Nguyen, Q. T.; Favre, E.; Ping, Z. H.; Néel, J. *J. Membr. Sci.* **1996**, *113*, 137−150.
(65) Ch'ng, L. C.; Samanta, A. K.; Czakó, G.; Bowman, J. M.; Reisler, H. *J. Am. Chem. Soc.* **2012**, *134*, 15430−15435.